

Real-time AFM diagrams on your Macintosh

Frank S. Spear

Department of Earth and Environmental Sciences, Rensselaer Polytechnic Institute
Troy, NY 12180 USA <spearf@rpi.edu>

(Received December 15, 1998; Published May 25, 1999)

Abstract

An algorithm is presented for the calculation of stable AFM mineral assemblages in the KFMASH system based on an internally consistent thermodynamic data set and the petrogenetic grid derived from this data set. The P-T stability of each divariant (three-phase) AFM assemblage is determined from the bounding KFASH, KMASH and KFMASH reactions. Macintosh regions (enclosed areas defined by a sequence of x-y points) are created for each divariant region. The Macintosh toolbox routine "PtInRgn" (point-in-region) is used to determine whether a user-specified P and T falls within the stability limit of each assemblage, and the compositions of minerals in the stable assemblages are calculated and plotted. Implementation of the algorithm is coded in FORTRAN as a module for program Gibbs (Spear and Menard, 1989). Users can calculate individual AFM diagrams at any P-T condition within the limits of the P-T grid, and sequences of AFM diagrams along any P-T path. Diagrams can be saved as PICT images for creating animations. The internally consistent thermodynamic data sets of Holland and Powell (1998) and Spear and Cheney (unpublished) are supported.

The algorithm and its implementation provide a useful tool for researchers to explore the implications of a petrogenetic grid and to compare predictions of different thermodynamic data sets. Comparison of natural samples with predictions from the grid can be made if appropriate projections of the natural data into the KFMASH system are made. Results are also useful to students learning to understand petrogenetic grids and the progressive metamorphism of pelitic mineral assemblages.

Keywords: AFM diagrams, petrogenetic grid, pelites, pelitic schists, thermodynamics, computing, Gibbs method, education, metamorphic petrology

Introduction

Since J. B. Thompson introduced the muscovite projection for metapelites over 40 years ago (Thompson, 1957), the AFM diagram (muscovite or Thompson projection) has been used extensively by petrologists for presentation of mineral assemblage and composition data of pelitic schists. Ultimately, the goal of constructing phase diagrams from natural mineral assemblages is to extract P-T information that can then be used to constrain the tectonic and thermal regime during metamorphism. The link between the graphical representation of a natural mineral assemblage (e.g. the AFM diagram) and P-T information is made by constructing petrogenetic grids for the chemical system of interest. The AFM diagram is successful because it is a fairly rigorous representation of the phase relations in the relatively complex system $\text{SiO}_2\text{-Al}_2\text{O}_3\text{-MgO-FeO-K}_2\text{O-H}_2\text{O}$

(KFMASH). This system is a good approximation of the chemical system of pelites, so petrogenetic grids for the KFMASH system form a useful basis for extracting P-T information.

Although changes in the topology of AFM diagrams are easily related to reactions on the KFMASH grid, changes in mineral composition that occur along univariant reactions and within divariant fields are not readily apparent from a grid. Calculations of stable mineral compositions are required if natural assemblages are to be compared with predictions from a grid. Examples of these calculations have been published (e.g. Symmes and Ferry, 1992; Powell, et al., 1998), but the algorithm described in this paper is designed so that users with little thermodynamic background can calculate quantitatively precise AFM phase diagrams. Its purpose is not to replace other methods, but rather to provide ready access to rigorous AFM diagrams for use in both research and teaching.

The algorithm

Calculation of the complete AFM diagram at a specified set of P-T conditions requires identification of the set of assemblages with the lowest free energies. The approach adopted here is to use the information inherent in a petrogenetic grid to provide the necessary information about the stable mineral assemblages.

Reactions in the KFMASH system delineate fields for AFM mineral compatibilities. Reactions that occur in the KFASH or KMASH chemical subsystems create or destroy one divariant KFMASH assemblage (on the AFM diagram, divariant assemblages are represented as three-phase triangles, and will be referred to as such). Reactions in the KFMASH system (tie-line flips or terminal stability reactions) create or destroy four, three-phase triangles. The stability field of every three-phase AFM triangle is bounded, therefore, by segments of KFASH, KMASH, or KFMASH reactions (not counting degenerate reactions such as the Al_2SiO_5 polymorphs) that extend between invariant points. Similarly, at every P-T point there will be a suite of stable 3-phase assemblages and 2-phase tie-lines.

Implementation of the algorithm begins with, therefore, a petrogenetic grid calculated from an internally consistent thermodynamic data set. Based on the grid, the P-T conditions of the bounding reactions and end points (either an invariant point or a pressure or temperature limit based on the extremities of the grid) for every three-phase assemblage are determined and stored in files.

To identify the suite of stable AFM assemblages at a specified P and T, the algorithm uses the Macintosh toolbox routine called PtInRgn (point-in-region) (Apple Computer, Inc., 1994), which returns true if a specified x-y point falls within a predefined region in x-y space. Regions are first created from the P-T stability information for each of the divariant AFM assemblages and each region is checked against the user specified P-T conditions with the toolbox call

```
isTrue = PtInRgn(myPoint, regionPointer).
```

A list is created of the stable assemblages, the compositions of the phases in each assemblage are calculated at the specified T and P, and the results are plotted on an AFM diagram. Two-phase tie-lines are also calculated.

As an example, the stable region of the assemblage garnet + biotite + chlorite + muscovite + quartz + H₂O in the KFMASH is shown on the grid constructed from the data set of Spear and Cheney (unpublished) in Figure 1. Each magenta dot shows a P-T coordinate on the boundary of the stability region for this assemblage, and the array of P-T points is used to define the Macintosh region for this assemblage, with each assemblage having a unique region that can be accessed by the region pointer. During execution, the function PtInRgn will return “true” if supplied with P-T coordinates within the defined region for that assemblage.

Thermodynamic data sets

Two thermodynamic data sets are currently supported in the program: Holland and Powell (1998) and Spear and Cheney (unpublished). Implementation of the Holland and Powell data set includes non-ideal activity models for pelitic minerals as specified in Holland and Powell (1998). The Spear and Cheney (unpublished) data set is an update of the data set published by Spear and Cheney (1989) that was developed specifically for the purpose of calculating a petrogenetic grid consistent with known parageneses in pelites. The data set includes enthalpies for common pelitic minerals and multi-site ideal ionic models for biotite, chlorite, and muscovite.

Implementation

The algorithm has been coded in FORTRAN as a module into program Gibbs (Spear and Menard, 1989; Spear et al., 1991). Options are provided that enable the user to calculate and to plot AFM diagrams at any desired P-T condition, and to examine how the stable mineral assemblages and the compositions of minerals in those assemblages evolve along any chosen P-T path. Options are available to adjust the appearance of the AFM diagrams by selection of the color of the tie lines and three-phase regions and to plot a small P-T grid as an inset on the AFM diagram to show location of the P-T point.

Four methods are provided for specifying the T and P of the calculations: (1) The user may input single T and P values; (2) The user may specify the starting P-T conditions and a value for ΔT and ΔP and generate a series of T-P conditions along a linear T-P path; (3) The user may select a T-P point by clicking on the petrogenetic grid; and (4) The user may specify the name of an input file that contains a list of T-P conditions, for example, along a P-T path of interest. Any T-P conditions within the limits of the calculated grid may be specified. The P-T point is labeled on the grid with a colored dot.

Generally, it is advantageous to erase an old AFM diagram before plotting a new one, but the option is provided to overwrite the AFM diagrams when it is desired to examine the shift in Fe/Mg as a function of changes in T and P. Figure 2 shows an example of this application for the assemblages garnet + biotite + Al₂SiO₅ (andalusite or sillimanite) and cordierite + biotite + Al₂SiO₅. As can be seen in the figure, along the same P-T path (600 - 670 °C, 3 - 5.1 kbar), the

Fe/Mg of the Crd + Bt + Als assemblage changes considerably more than that of the assemblage Grt + Bt + Als.

The option is also provided to show the compositional shifts of a three-phase assemblage without regard as to whether the assemblage is stable. This option is useful to examine the P-T-X shift of a three-phase assemblage over the entire KFMASH composition range.

A particularly useful tool is the ability to display the P-T stability region of any 3-phase assemblage on the petrogenetic grid. As an example, the stability regions of two, three-phase assemblages (garnet + staurolite + biotite and staurolite + chlorite + sillimanite) are shown in Figure 3. The peak metamorphic P-T conditions of an outcrop that produced samples with these two assemblages would be restricted to the relatively small P-T region of overlap shown on Figure 3.

Individual AFM diagrams may be saved as PICT images with a sequential number added to the file name. These PICT files will thus be sorted in the Macintosh Finder, permitting easy loading into programs for the creation of animated Gif files or Quicktime movies. A simple method of creating an animation is to save the PICT files in a separate folder and then load into NIH Image (developed at the U.S. National Institute of Health and available on the Internet at <http://rsb.info.nih.gov/nih-image/>; Rasband, 1997). The separate images can then be converted into a stack (Windows to Stack option) for viewing as an animation or saving as a Quicktime movie. Examples of movies are presented below.

A simplified example

An example of the operation and output of the algorithm for calculation of AFM diagrams is presented in Figure 4. The static figure shows an AFM diagram calculated using the thermodynamic data and petrogenetic grid of Spear and Cheney (unpublished). An interactive version of this figure is available as an html image map by clicking the text in the figure caption. This figure is designed to illustrate the ease with which AFM diagrams can be displayed for any P-T condition. The figure is a pale shadow of the Gibbs algorithm, however, inasmuch as it merely displays an image of an AFM diagram that has already been calculated, and only a single AFM diagram is available for each P-T region. Within program Gibbs, the user can select any P-T point over the entire grid and examine the shifts in mineral compositions within divariant regions as well as the change in AFM topology between regions. For example, a Quicktime movie is presented in Figure 5 that illustrates the sequence of AFM diagrams calculated within an individual P-T region along a heating and loading path from 604 °C, 2684 bars to 676 °C, 5859 bars. The considerable shift in Fe/Mg, which is not displayed in Figure 4, is readily observable in the movie.

Comparison of thermodynamic data sets

A second example is presented in Figure 6, which contains two movies of sequences of AFM diagrams calculated from the thermodynamic data sets of Holland and Powell (1998) and Spear and Cheney (unpublished) along the same P-T path. Comparison of the two movies and associated petrogenetic grids reveals similarities and differences in the predicted stability fields of important pelite mineral assemblages.

Similarities between the grids.

- (1) Both grids correctly predict the parageneses observed in Barrovian facies series.
- (2) Both grids have a field for the problematic assemblage chloritoid + biotite at low pressure and temperature, although the size of the field on the Spear and Cheney grid is larger.
- (3) For the most part, both grids predict the correct partitioning between Fe-Mg silicates.

Differences between the grids.

- (1) The Holland and Powell (H&P) grid places the Al_2SiO_5 triple point at approximately 505 °C, 3.9 kbar whereas the Spear and Cheney (S&C) grid places the triple point at approximately 550 °C, 4.6 kbar. The H&P triple point is consistent with experiments by Holdaway (1971); S&C opted to place the andalusite = sillimanite reaction at higher temperature to permit a stability field for andalusite migmatites (following the arguments of Pattison, 1992).
- (2) The H&P grid predicts that the controversial assemblage staurolite + cordierite + muscovite is not stable, consistent with the analysis of natural parageneses by Pattison et al. (in press). The S&C grid incorrectly predicts a stability field for this assemblage.
- (3) In detail, the predicted Fe-Mg partitioning between certain silicates is problematic on both grids. The S&C data set predicts Fe-Mg partitioning between biotite and cordierite that is more pronounced than that observed in nature. The H&P data set predicts that the Fe/Mg of staurolite is higher than the garnet + Al_2SiO_5 tie-line and the Fe/Mg of chlorite is less than the biotite + cordierite tie-line, in contrast to observations from natural assemblages.
- (4) The H&P data set places the KFASH reaction almandine + muscovite = biotite + Al_2SiO_5 at approximately 4 kbar, which is inconsistent with the observation of garnet + biotite + andalusite or sillimanite assemblages with $\text{Fe}/(\text{Fe} + \text{Mg})$ in garnet = 0.93.
- (5) The slope of the KMASH (and divariant KFMASH) reaction cordierite + muscovite = biotite + Al_2SiO_5 is negative in the S&C grid and positive in the H&P grid. Pattison and Tracy (1991) have presented strong arguments based on natural parageneses that this reaction should have a negative slope.

In summary, although both grids correctly portray the major parageneses observed in pelitic rocks, both grids make certain predictions that are inconsistent with observations on natural samples. It should be noted as well that neither grid incorporates melting, and that many of the reactions above approximately 650 °C will be metastable with respect to melting reactions.

Discussion

The algorithm presented here makes use of the thermodynamic stability information inherent in a petrogenetic grid to determine the suite of stable assemblages at specified P-T conditions, thus obviating the need for extensive testing for stability during phase diagram construction. Implementation of the algorithm has been designed primarily for ease of end-user use, but it is important to point out that considerable pre-processing is required to first calculate the petrogenetic grid and to index the stability regions of each stable assemblage. However, once this is complete, only a minimum of sorting is required to compile a list of stable assemblages, and calculation of the stable assemblages on the AFM projection can proceed by standard methods of solving the

simultaneous non-linear equilibrium equations. The result is an efficient algorithm that achieves the specific goal of real-time calculation of phase diagrams on a desktop computer.

Similar methods have been used by other authors for the calculation of phase diagrams. The approach of Worley and Powell (1998) and Powell et al. (1998) is to calculate the compositions of phases along univariant reactions and to interpolate the compositions in the divariant regions between reactions to produce a sequence of AFM diagrams and Quicktime movies. Symmes and Ferry (1992) present calculated phase diagrams using similar non-linear equation sets but do not specify how graphical output was achieved.

Other approaches have been presented for calculation of phase diagrams and some of the more general methods are summarized by Connolly (1990). A robust algorithm has been described by Connolly and Kerrick (1987) and Connolly (1990) and is incorporated into the computer program Vertex. An alternative approach to the calculation of phase diagrams was presented by De Capitani and Brown (1987) and is implemented in the program Theriak. These approaches are far more general in that no *a priori* knowledge of the stable mineral assemblage is required for the calculation of phase diagrams.

Research applications

An obvious application of the algorithm described here is the comparison of phase diagrams constructed from thermodynamic data sets. Developers of thermodynamic data bases will therefore have an option for presentation of results that is readily accessible to a wide range of users, and researchers will have a simple means of comparing the consequences of different choices of thermodynamic data.

Another application of this tool is exploration of the reactions that may affect a specific bulk composition during progressive metamorphism. Both discontinuous and continuous reactions may be responsible for the appearance or disappearance of a phase, and examination of the sweep of 3-phase triangles with changing P-T conditions is a means of evaluating the relative importance of each for a rock. Examination of AFM diagrams in this way complements the information obtained from pseudosections, in which stability regions for individual bulk compositions are outlined on intensive variable diagrams (e.g. Powell et al., 1998).

Application to natural samples: Thermobarometry. Comparison of calculated AFM diagrams to those inferred from natural samples has application for the determination of metamorphic P-T conditions. However, under most circumstances, direct comparison must be done with care because natural samples contain extra components that alter the stability of minerals relative to the KFMASH subsystem. Fortunately, methods are available that permit rigorous calculation of the compositions of minerals in a chemical subsystem based on the measured compositions in the sample.

The issue of recalculating natural assemblages to plot on AFM diagrams has been addressed by Spear (1988), and will be briefly summarized here. Consider the assemblage garnet + biotite + sillimanite + quartz + muscovite in which the garnet contains considerable spessartine component. It is commonly assumed that the Fe/Mg of biotite (or other Fe-Mg solid solutions) is not affected

by the MnO content of garnet because these minerals do not contain appreciable MnO. This assumption is incorrect, as can be seen in a sillimanite projection onto the plane Fe-Mg-Mn (Fig. 7). With increasing Mn content in garnet, the Fe/Mg of garnet *and* biotite decrease (see also, Albee, 1964 who was apparently the first to recognize this fact). For the purposes of plotting an AFM diagram for comparison with a calculated diagram in the KFMASH system, the correct compositions of garnet and biotite are those labeled with open circles (Fig. 7). Other methods of calculating the plotting positions of garnet and biotite on the AFM diagram such as lumping Mn with Fe (or Mg), preserving the Fe/Mg, or the “least squares” solution, can be seen to result in plotting positions that inaccurately reflect the KFMASH phase relations.

The thermodynamic basis for the projection is preservation of the values of the equilibrium constants defined for all independent equilibria in the natural assemblage. The compositions of minerals are calculated with values of the equilibrium constant held constant in the limit where the MnO (or CaO etc.) content of the phases is zero. Examples are provided by Spear (1988) for projecting phase compositions in the MnKFMASH system into the KFMASH system and by Spear and Markussen (1997) for projection of the compositions of coexisting ortho- and clinopyroxenes onto the pyroxene quadrilateral, with large effect on the inferred temperatures based on the pyroxene solvus.

An example of these calculations is shown in Figure 8 using data from Hodges and Spear (1982) from Mt. Moosilauke, New Hampshire. Inferred P-T conditions are slightly lower pressure than the Al_2SiO_5 triple point and near the andalusite-sillimanite boundary. Garnets from these rocks contain 14-21 mole % spessartine. Calculations were performed using program Gibbs with the compositions of minerals in the natural assemblage at the inferred P and T of equilibration used as input. Spessartine, T and P were chosen as independent variables, the system was iterated at constant T and P to where $X_{\text{sps}} = 0$, and the resulting AFM diagrams plotted.

Comparison of the two AFM diagrams for these data reveals a substantial shift towards higher Fe/Mg in the projected plot (Fig. 8b). Calculated AFM diagrams for the two sets of mineral compositions (Fig. 8c) reveal that the pressure of equilibration would have been overestimated by nearly 2 kbar had the thermodynamic projection not been used. The inferred P-T conditions using the projected compositions (545 °C, 4688 bars) are consistent with the regional setting, which is inferred to be near the Al_2SiO_5 triple point (Rumble, 1973; Hodges and Spear, 1982).

Instructional applications

Students learning metamorphic petrology are instructed in the use of AFM diagrams to illustrate pelitic mineral assemblages and to show the ways in which these diagrams change with changing P-T conditions. In the author's experience, there are three hurdles students must overcome before AFM diagrams may be utilized for evaluating P-T evolution. The first is understanding how the stable mineral assemblages on the AFM diagram change as reactions in the KFMASH, KFMASH and KFMASH systems are crossed (changes in topology). Exercises requiring students to construct sequences of AFM diagrams along specified P-T trajectories are useful for acquiring this ability. The second is appreciating the change in Fe/Mg for individual three-phase assemblages as P and T change through divariant regions. T-X and P-X constructions are useful to illustrate this point, but it is difficult for students to fully appreciate the relationships between the P-T, T-X, P-X and AFM

diagrams. The third is assessing the P-T stability limits of a particular three-phase assemblage, and the P-T constraints imposed by a set of three-phase assemblages (the entire AFM topology).

Three interactive exercises have been used in classes by the author with the goal of helping students understand the relationship between mineral assemblages, petrogenetic grids, and phase diagrams.

- (1) Provide the student with an unlabeled version of the petrogenetic grid and, using the program, require the student to label the reactions based on the change in the phase diagram topology. This can readily be accomplished with the option to click on the grid to obtain the AFM diagram (e.g. Fig. 4).
- (2) Provide the student with a list of assemblages (e.g. an entire AFM topology) and ask the student to determine the range of P-T conditions consistent with the suite of mineral assemblages. This can readily be accomplished with the option to outline the reactions that define the stability region of an assemblage (e.g. Fig. 3).
- (3) Specify a bulk composition (a point that plots on the AFM diagram) and require the student to give the paragenesis of that bulk composition over a prescribed P-T path. This could be accomplished interactively by clicking on the grid, or by first making a movie of AFM diagrams along the P-T path. An important aspect of this exercise is that some phase changes will be the consequence of univariant reactions, whereas others will result from changes of mineral composition (e.g. Fe/Mg) in divariant regions. The student could also be asked to predict the Fe/Mg zoning that would be observed in garnet along the prescribed path or how the composition of a mineral included in garnet (e.g. biotite) will differ from the composition of biotite in the matrix (at the peak T and P).

Conclusions

The power of this algorithm is its ease of use. AFM diagrams based on a thermodynamic data set can be calculated on a desktop computer and sequences of AFM diagrams can be calculated along any P-T path. Changes in Fe/Mg of phases with changing P-T conditions are readily viewed, as are the limiting reactions that bound the P-T stability of individual assemblages. The interactive capabilities render this algorithm useful as both a research and teaching tool.

Acknowledgments

This work was supported, in part, by funding from the National Science Foundation (EAR-9706403 to FSS). Jack Cheney is warmly thanked for innumerable discussions about pelites and for substantially improving the presentation. Helpful reviews were also supplied by J. Connolly and B. Worley.

References

- Albee, A.L. (1964) Distribution of Fe, Mg, and Mn between garnet and biotite in natural mineral assemblages. *Journal of Geology*, 73, 155-164.
- Apple Computer, Inc. (1994) *Inside Macintosh: Imaging With QuickDraw*, 832 p. Addison-Wesley Publishing Company, Reading, MA.
- Connolly, J.A.D. (1990) Multivariable phase diagrams: An algorithm based on generalized thermodynamics. *American Journal of Science*, 290, 666-718.
- Connolly, J.A.D., and Kerrick, D.M. (1987) An algorithm and computer program for calculating composition phase diagrams. *CALPHAD*, 1, 1-55.
- de Capitani, C., and Brown, T.H. (1987) The computation of chemical equilibrium in complex systems containing non-ideal solutions. *Geochimica et Cosmochimica Acta*, 51, 2639-2652.
- Hodges, K.V., and Spear, F.S. (1982) Geothermometry, geobarometry and the Al_2SiO_5 triple point at Mt. Moosilauke, New Hampshire. *American Mineralogist*, 67, 1118-1134.
- Holdaway, M.J. (1971) Stability of andalusite and the aluminum silicate phase diagram. *American Journal of Science*, 271, 97-131.
- Holland, T.J.B., and Powell, R. (1998) An internally-consistent thermodynamic dataset for phases of petrological interest. *Journal of Metamorphic Geology*, 16, 309-343.
- Pattison, D.R.M. (1992) Stability of andalusite and sillimanite and the Al_2SiO_5 triple point: constraints from the Ballachulish aureole, Scotland. *Journal of Geology*, 100, 423-446.
- Pattison, D.R.M., Spear, F.S., and Cheney, J.T. (in press) Polymetamorphic origin of muscovite + staurolite + cordierite + biotite assemblages: Implications for metapelitic petrogenetic grids and P-T paths. *Journal of Metamorphic Geology*.
- Pattison, D.R.M., and Tracy, R.J. (1991) Phase equilibria and thermobarometry of metapelites. In D.M. Kerrick, Ed., *Contact Metamorphism*, 26, p. 105-206. Mineralogical Society of America, Washington, D. C.
- Powell, R., Holland, T., and Worley, B. (1998) Calculating phase diagrams involving solid solutions via non-linear equations, with examples using THERMOCALC. *Journal of Metamorphic Geology*, 16, 576-588.
- Rasband, W. (1997) NIH Image, National Institutes of Health, Washington D. C. (<http://rsb.info.nih.gov/nih-image/>)
- Rumble, D., III (1973) Andalusite, kyanite, and sillimanite from the Mount Moosilauke region, New Hampshire. *Geological Society of American Bulletin*, 84, 2423-2430.
- Spear, F.S. (1988) Thermodynamic projection and extrapolation of high-variance mineral assemblages. *Contributions to Mineralogy and Petrology*, 98, 346-351.
- Spear, F.S., and Cheney, J.T. (1989) A petrogenetic grid for pelitic schists in the system SiO_2 - Al_2O_3 - FeO - MgO - K_2O - H_2O . *Contributions to Mineralogy and Petrology*, 101, 149-164.
- Spear, F.S., and Markussen, J.C. (1997) Mineral zoning, P-T-X-M phase relations, and metamorphic evolution of some Adirondack granulites, New York. *Journal of Petrology*, 38, 757-783.
- Spear, F.S., and Menard, T. (1989) Program GIBBS: A generalized Gibbs method algorithm. *American Mineralogist*, 74, 942-943.
- Spear, F.S., Peacock, S.M., Kohn, M.J., Florence, F.P., and Menard, T. (1991) Computer programs for petrologic P-T-t path calculations. *American Mineralogist*, 76, 2009-2012.

- Symmes, G.H., and Ferry, J.M. (1992) The effect of whole-rock MnO content on the stability of garnet in pelitic schists during metamorphism. *Journal of Metamorphic Geology*, 10, 221 - 237.
- Thompson, J.B., Jr. (1957) The graphical analysis of mineral assemblages in pelitic schists. *American Mineralogist*, 42, 842-858.
- Worley, B., and Powell, R. (1998) Making movies: Phase diagrams changing in pressure, temperature, composition and time. In P.J. Treloar, and P.J. O'Brien, Eds., *What Drives Metamorphism and Metamorphic Reactions?*, p. 269-280. Geological Society of London Special Publications, 138, London.
- Worley, B., and Powell, R. (1998) Singularities in NCKFMASH (Na₂O-CaO-K₂O-FeO-MgO-Al₂O₃-SiO₂-H₂O). *Journal of Metamorphic Geology*, 16, 169-188.

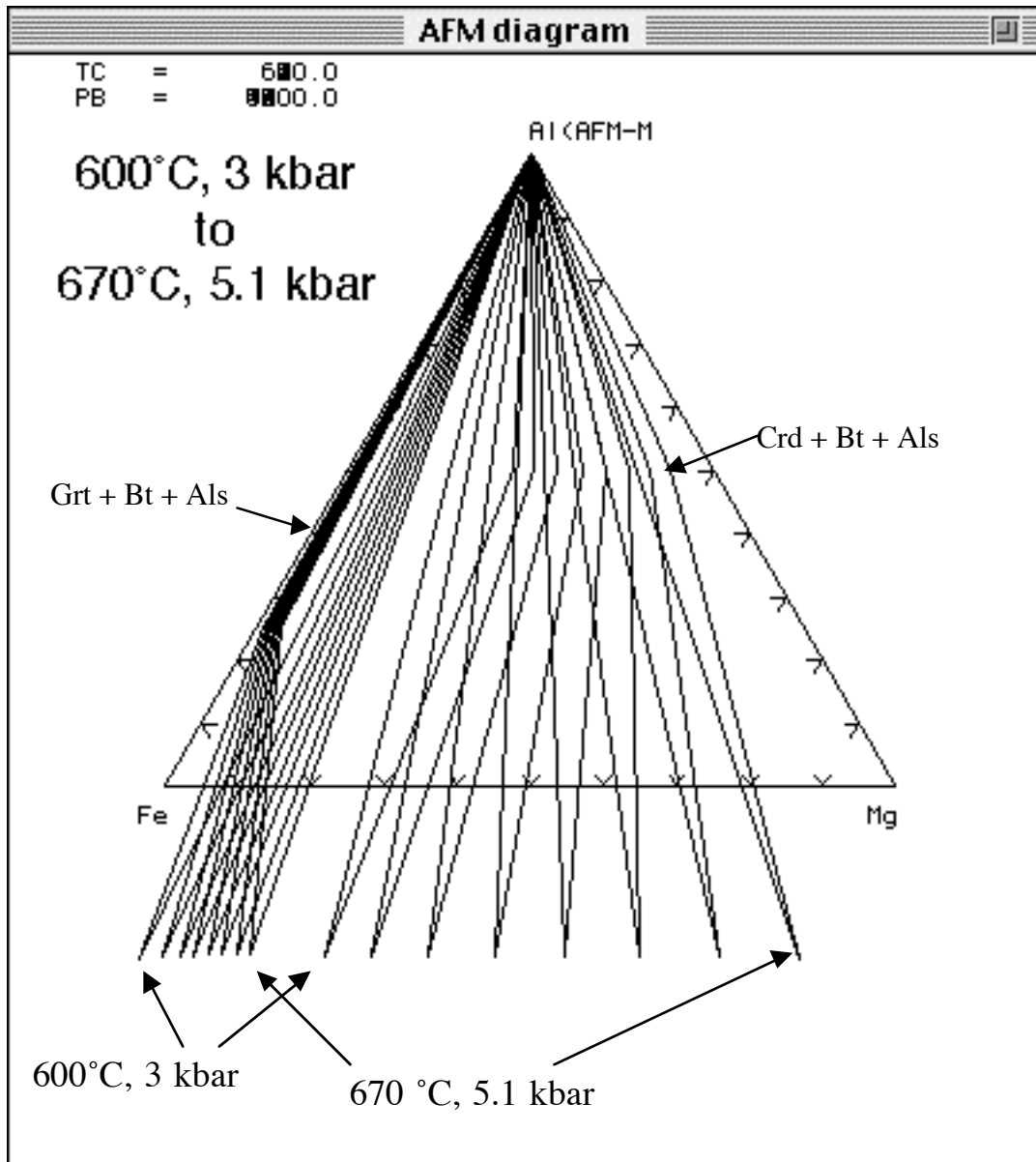


Figure 2. Sets of overlapping three-phase triangles for the assemblage garnet + biotite + Al_2SiO_5 (andalusite or sillimanite) and cordierite + biotite + Al_2SiO_5 generated by suppressing the “erase old plot” option. For the same change in T and P, the shift of Fe/Mg in the assemblage Crd + Bt + As is considerably greater than that of the assemblage Grt + Bt + Als.

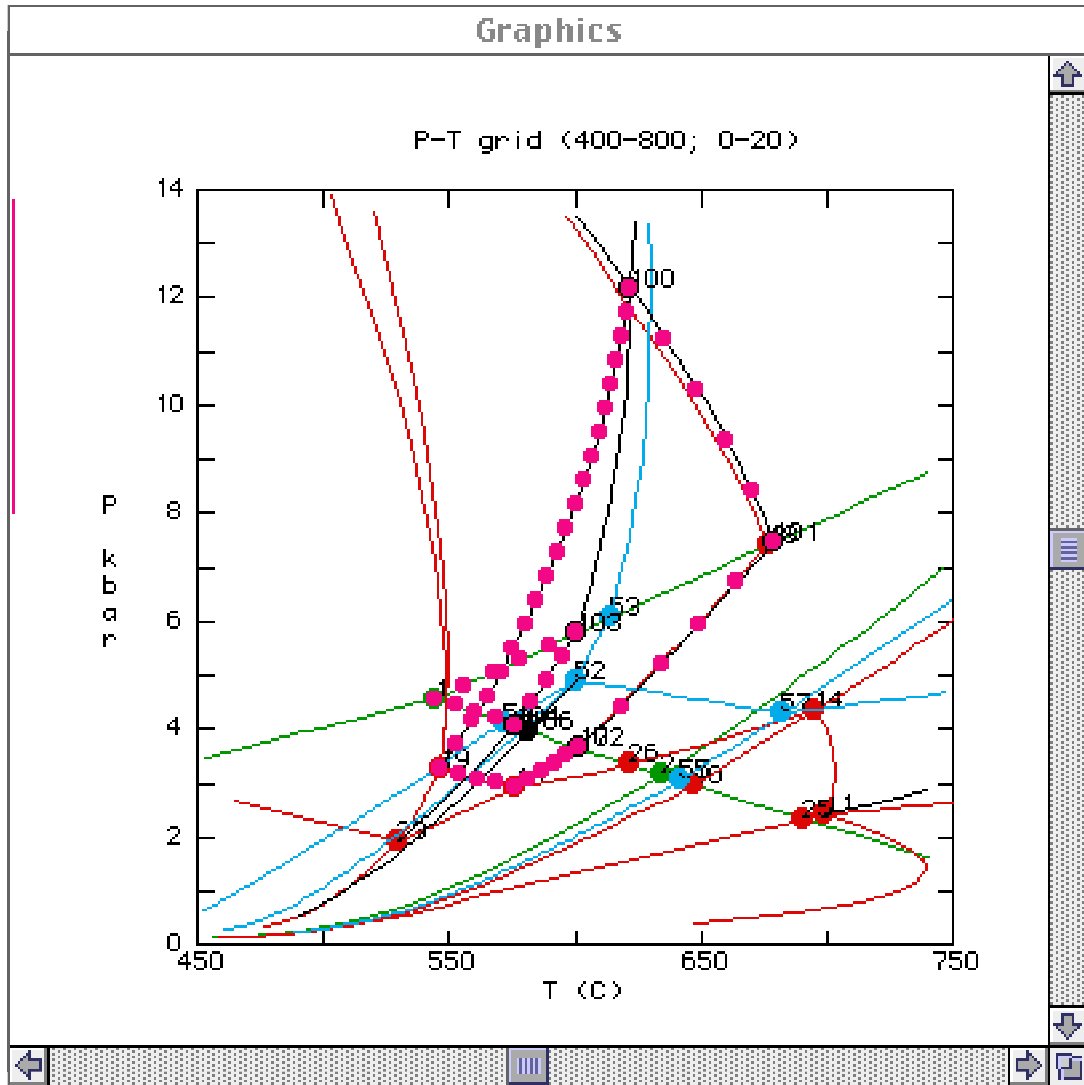


Figure 3. P-T grid showing the P-T points (magenta dots) that identify the boundaries of the P-T regions for the assemblages garnet + staurolite + biotite and staurolite + chlorite + sillimanite. A program option can be used to display similar illustrations for every stable divariant assemblage.

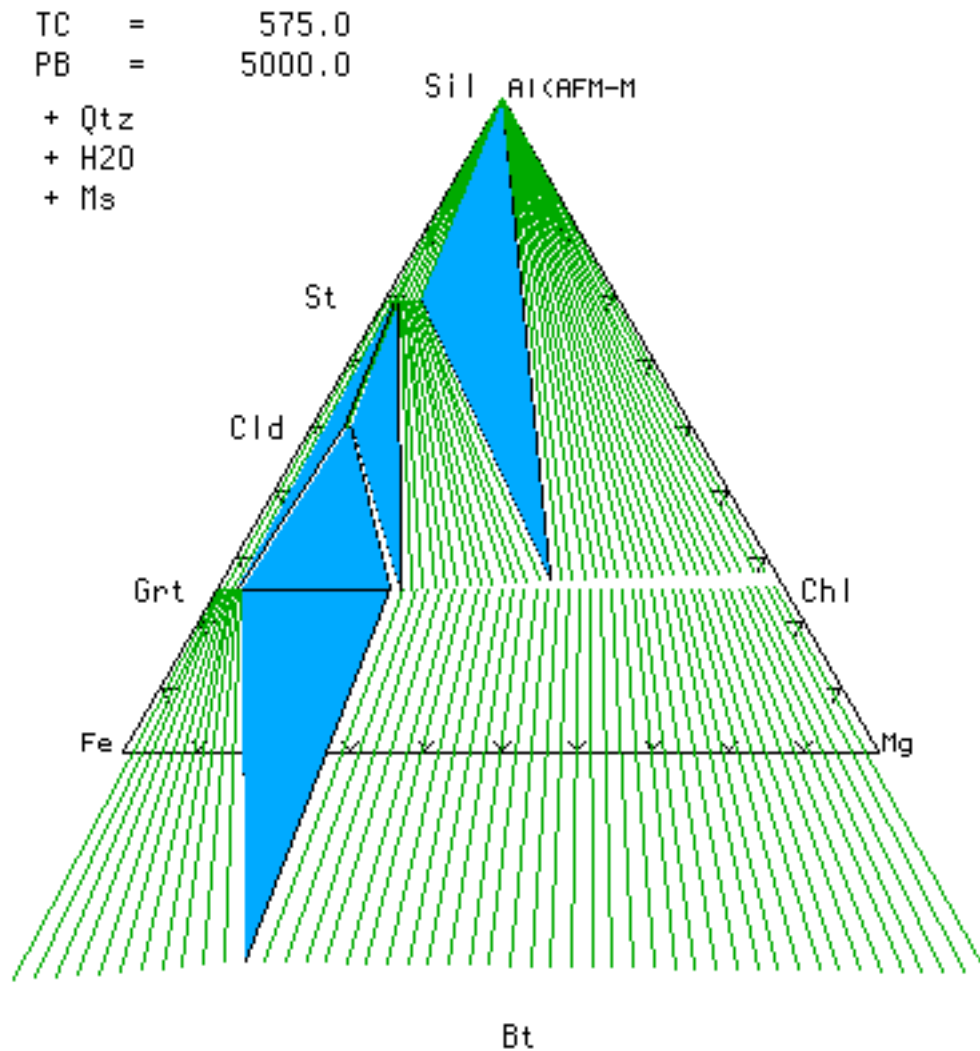


Figure 4a. AFM diagram calculated at 575 °C, 5 kbar based on the thermodynamic data and petrogenetic grid of Spear and Cheney (unpublished). An interactive version of this figure that incorporates an html image map and “point and click” for selection of P-T regions is available by clicking here: [“point-and-click interactive figure”](#). Display of the image will require opening a browser window.

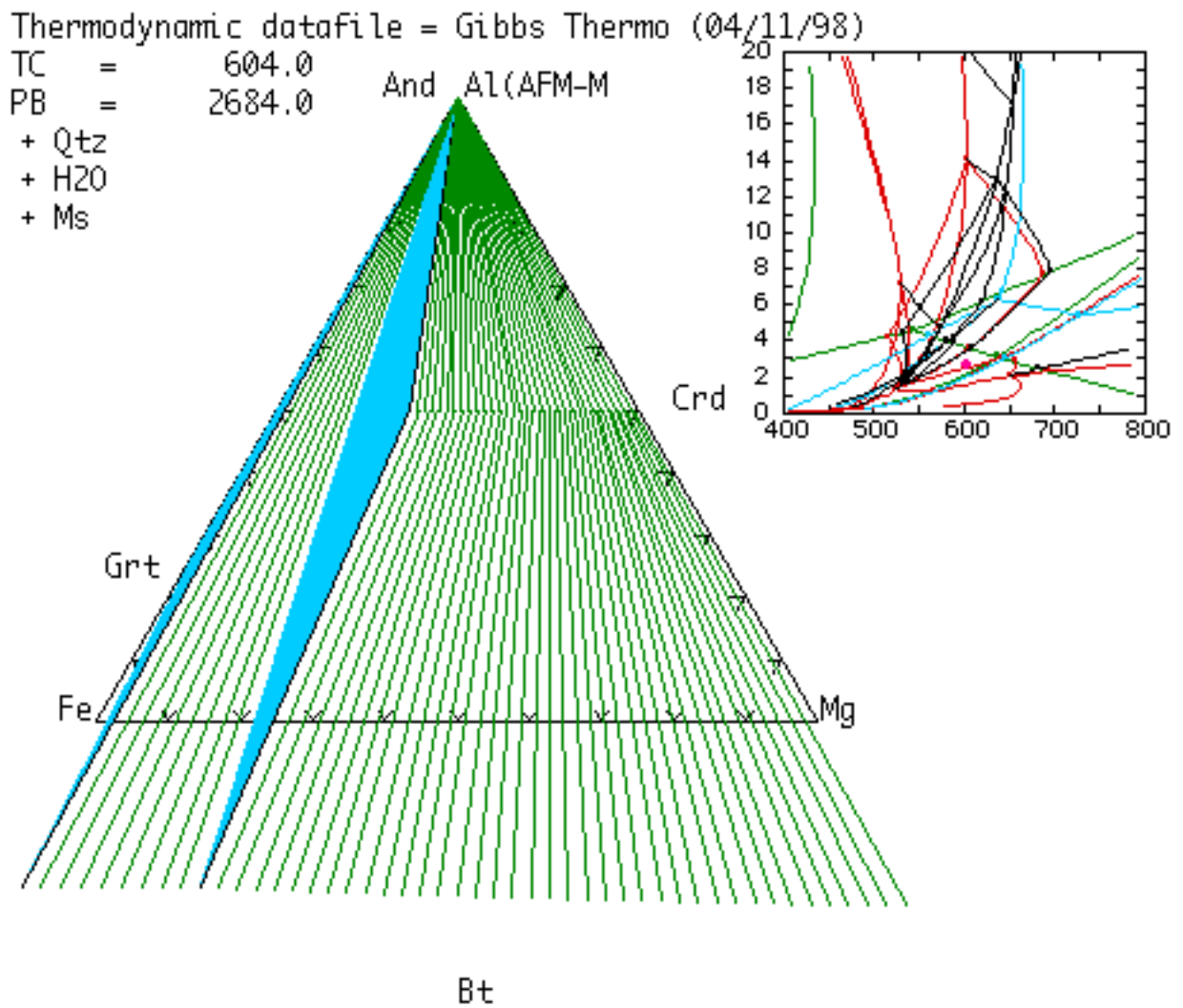


Figure 5. Quicktime movie depicting sequence of AFM diagrams within a single P-T region (604 °C, 2684 bars to 676 °C, 5859 bars) to illustrate the changes in Fe/Mg that are calculated within individual divariant regions. The movie is activated by clicking on the image.

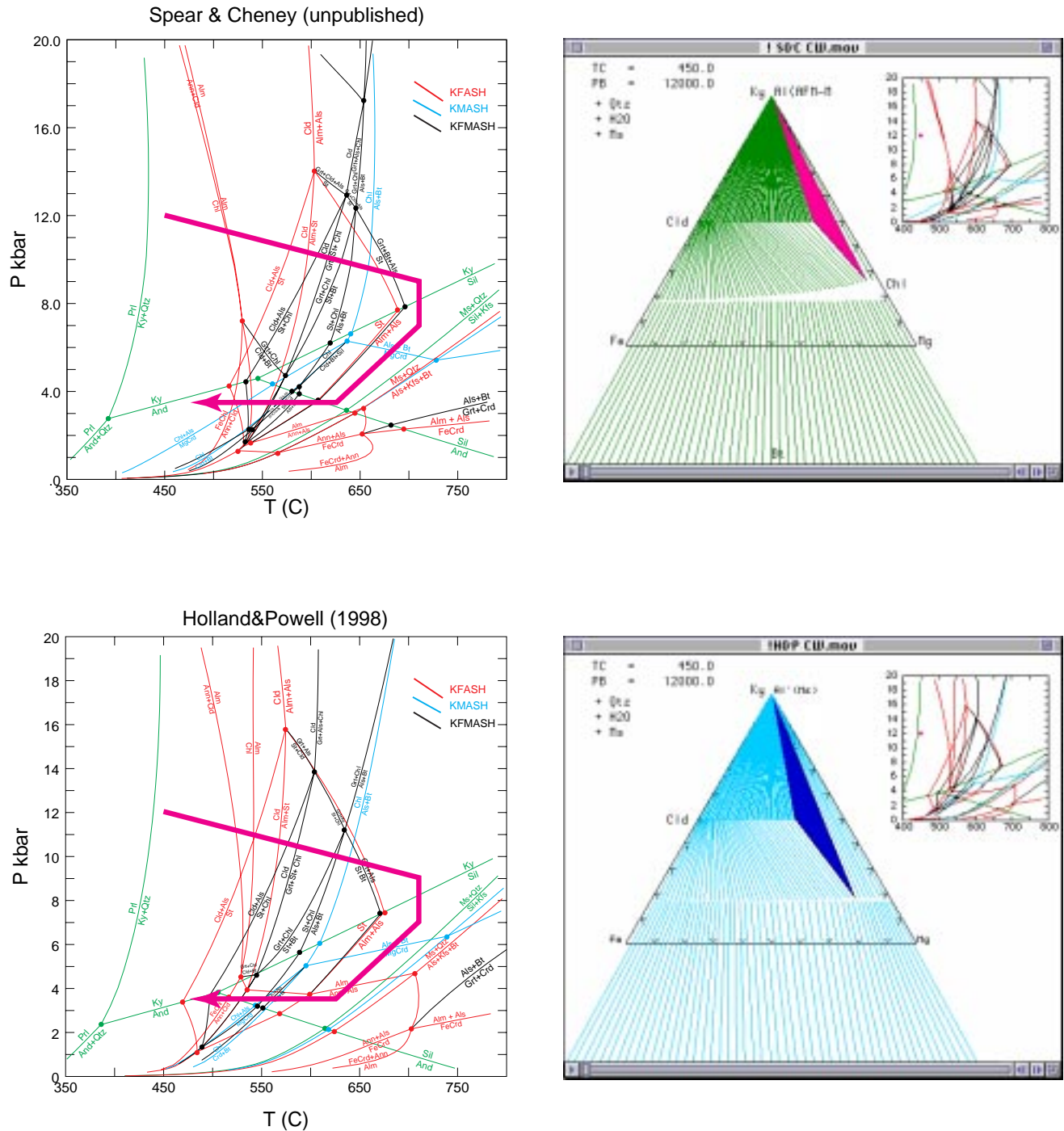


Figure 6. Petrogenetic grids and quicktime movies depicting sequences of AFM diagrams calculated from the thermodynamic data sets of (a) Spear and Cheney (unpublished) and (b) Holland and Powell (1998). The P-T path is clockwise and a prograde Barrovian sequence can be examined by viewing the movies in the forward direction and a prograde Buchan sequence examined by viewing the last part of the movies backwards. The movies are activated by clicking on the images.

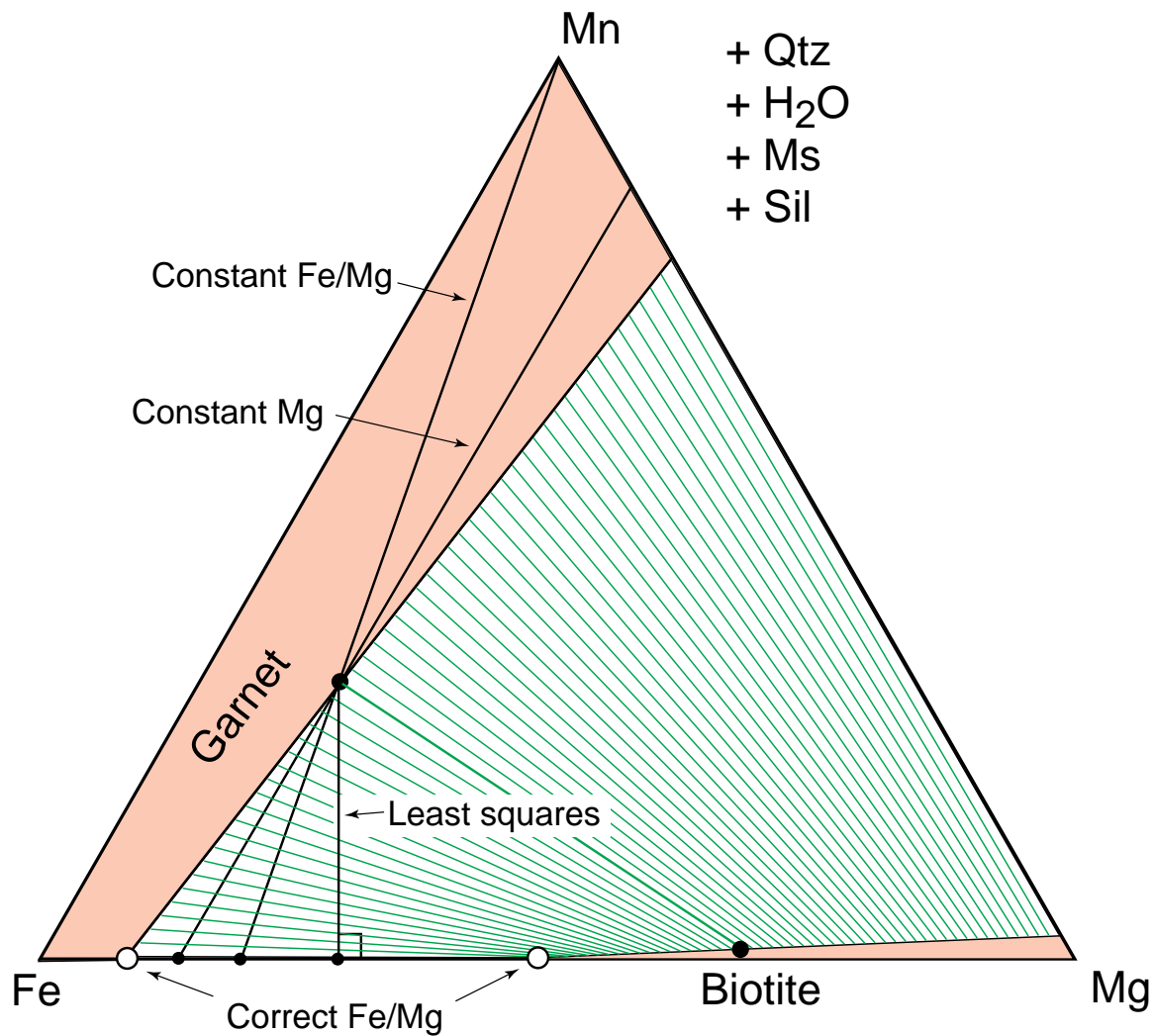


Figure 7. Projection from quartz, H_2O , muscovite, and sillimanite onto the plane Fe-Mg-Mn of the assemblage garnet + biotite + sillimanite + quartz + muscovite with variable Mn contents in garnet. The large black dots (garnet and biotite) represent the natural mineral pair to plot on an AFM diagram. Three construction lines show the effect of ignoring Mn (constant Fe/Mg), lumping Mn + Fe (constant Mg), and dropping a normal to the Fe-Mg join (least squares). The correct projection of the garnet - biotite pair into the KFMASH system is shown by the two open circles.

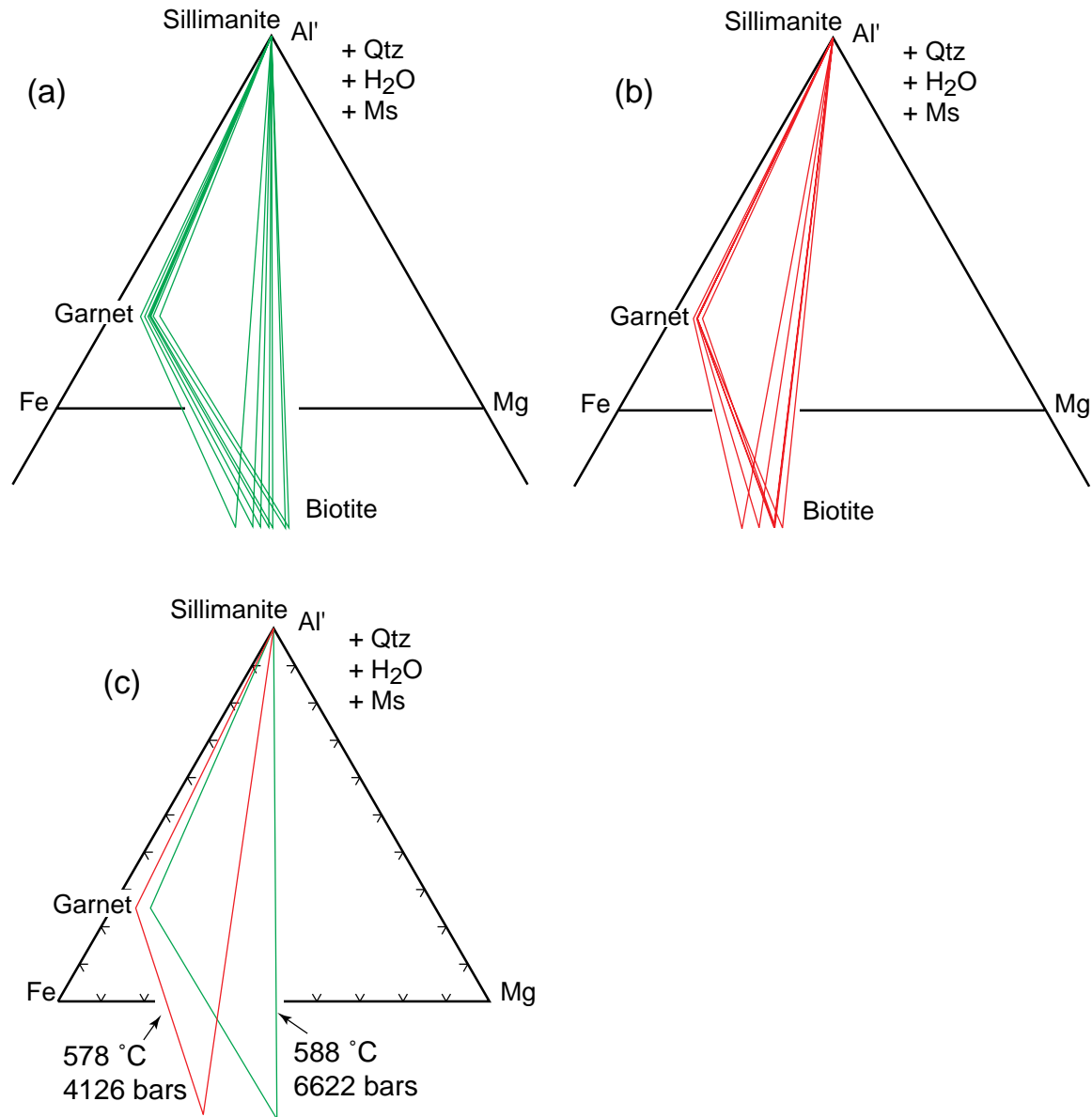


Figure 8. AFM diagrams for the assemblage garnet + biotite + sillimanite + muscovite + quartz. Data from Mt. Moosilauke, New Hampshire from Hodges and Spear (1982). (a) AFM diagram calculated by ignoring MnO and CaO in garnet and preserving Fe/Mg in garnet and biotite. (b) AFM diagram calculated by projecting the compositions of biotite and garnet onto the KFMASH plane using the method described in the text. Note that garnet plots at slightly higher Fe/Mg and that biotite Fe/(Fe + Mg) are as much as 0.12 higher in projection. (c) Calculated AFM triangles for the average garnet and biotite compositions shown in (a) and (b). P-T conditions inferred from the petrogenetic grid consistent with these compositions are listed with each triangle.